

Article

Effects of Superparamagnetic Nanoparticle Clusters on the Polymerase Chain Reaction

Toshiaki Higashi *, Hiroaki Minegishi, Yutaka Nagaoka, Takahiro Fukuda, Akinobu Echigo, Ron Usami, Toru Maekawa and Tatsuro Hanajiri

Bio-Nano Electronics Research Centre, Toyo University, 2100 Kujirai, Kawagoe, Saitama 350-8585, Japan; E-Mails: minehiro@toyo.jp (H.M.); nagaoka@toyo.jp (Y.N.); taka_f@toyo.jp (T.F.); echigo@toyo.jp (A.E.); usami_r@toyo.jp (R.U.); maekawa@toyo.jp (T.M.); hanajiri@toyo.jp (T.H.).

* Author to whom correspondence should be addressed; E-Mail: higashi162@toyo.jp; Tel.: +81-49-239-1375; Fax: +81-49-234-2502.

Received: 16 February 2012; in revised form: 19 March 2012 / Accepted: 23 March 2012 /

Published: 2 April 2012

Abstract: The polymerase chain reaction (PCR) method is widely used for the reproduction and amplification of specific DNA segments, and a novel PCR method using nanomaterials such as gold nanoparticles has recently been reported. This paper reports on the effects of superparamagnetic nanoparticles on PCR amplification without an external magnetic field, and clarifies the mechanism behind the effects of superparamagnetic particle clusters on PCR efficiency by estimating the structures of such clusters in PCR. It was found that superparamagnetic nanoparticles tend to inhibit PCR amplification depending on the structure of the magnetic nanoparticle clusters. The paper also clarifies that Taq polymerase is captured in the spaces formed among magnetic nanoparticle clusters, and that it is captured more efficiently as a result of their motion from heat treatment in PCR thermal cycles. Consequently, Taq polymerase that should be used in PCR is reduced in the PCR solution. These outcomes will be applied to novel PCR techniques using magnetic particles in an external magnetic field.

Keywords: magnetic nanoparticle; superparamagnetic; DNA; polymerase chain reaction; Taq polymerase

1. Introduction

The polymerase chain reaction (PCR) is a technique that allows reproduction and amplification of specific DNA segments using DNA polymerase *in vitro* [1]. Currently, the PCR method is widely used in genetic technology, bioscience, diagnosis therapy, medicine development and personal identification. Recently, it has been reported that PCR efficiency is improved by nanoparticles such as single-walled carbon nanotubes (SWCNTs), multi-walled carbon nanotubes (MWCNTs), carbon nanopowder, metallic nanoparticles and nonmetallic nanoparticles [2–5]. Among the variety of nanoparticles used, gold nanoparticles have been reported to have an outstanding effect on PCR efficiency. Li *et al.* [6] reported that such nanoparticles inhibited nonspecific products in PCR at low annealing temperatures. Li *et al.* [7] also reported that PCR efficiency was dramatically increased by using gold nanoparticles in PCR reagents. They speculate that the outstanding heat transfer properties of gold nanoparticles would enhance PCR efficiency and shorten reaction times. However, there have been a number of contradictory reports stating that gold nanoparticles have remarkably negative effects on PCR efficiency. Yang *et al.* [8] reported that they could inhibit PCR efficiency at high levels of concentration, and suggested a complex interaction between gold nanoparticles and the Taq polymerase DNA synthetic enzyme. Vu *et al.* [9] concluded that the surface interaction between gold nanoparticles and polymerase, rather than the DNA template or primers, inhibited PCR efficiency. They also demonstrated that the effects of gold nanoparticles on PCR could be reversed by increasing polymerase concentration or by adding bovine serum albumin (BSA) as a competitive displacer. Wan *et al.* [10] suggested that larger gold nanoparticles have a stronger inhibitory effect on PCR than smaller ones at the same particle concentration. According to their reports, the interaction between Taq polymerase and nanoparticle surfaces is one of the most significant factors in inhibiting PCR efficiency. The mechanism of PCR efficiency enhancement by several types of nanoparticles is currently attracting attention as a possible future-generation PCR technique using nanoparticles.

However, so far, there have been no reports on the effects of magnetic nanoparticles on PCR efficiency. Like gold nanoparticles, magnetic nanoparticles are dispersed in a solvent, forming a colloidal system. They have outstanding magnetic properties, and are classified into two types: ferromagnetic and paramagnetic/superparamagnetic. As ferromagnetic systems are magnetized, the particles tend to aggregate and form clusters, while paramagnetic/superparamagnetic systems remain stable in the absence of an external magnetic field [11–13]. The structure and magnetization of ferromagnetic and paramagnetic particles can be changed by applying external magnetic fields [14–16]. Also in the same way as gold nanoparticles, the surface of magnetic nanoparticles can be modified with a variety of chemicals and biomolecules. Mizuki *et al.* [17] leveraged the physical and chemical properties of magnetic nanoparticles, and reported that the enzyme activities of α -amylase immobilized on superparamagnetic particles increased in a rotational magnetic field. Magnetic nanoparticles can be utilized in the field of bio-nano technology, e.g., in the enhancement of magnetic resonance imaging (MRI), the development of drug delivery systems (DDSs), diagnosis therapies such as hyperthermia, and the labeling of tumor cells [18–20].

In this paper, we report on the effects of superparamagnetic nanoparticles on PCR amplification without an external magnetic field. We focus not only on the surface interaction between individual magnetic nanoparticles and PCR reagents, but also on the structures of magnetic particle clusters

transformed by heat treatment in conventional PCR thermal cycles. Here, we detail the effects of superparamagnetic nanoparticles on PCR amplification using several types of such nanoparticles with different surface treatments. We also clarify the mechanism behind the effects of superparamagnetic particle clusters on PCR efficiency from an estimation of their structures in PCR thermal cycles. Elucidation of the effect of magnetic nanoparticles on PCR amplification can be utilized to create novel PCR models exhibiting excellent magnetic properties and self-organization of the magnetic nanoparticles under an external magnetic field.

2. Experimental Section

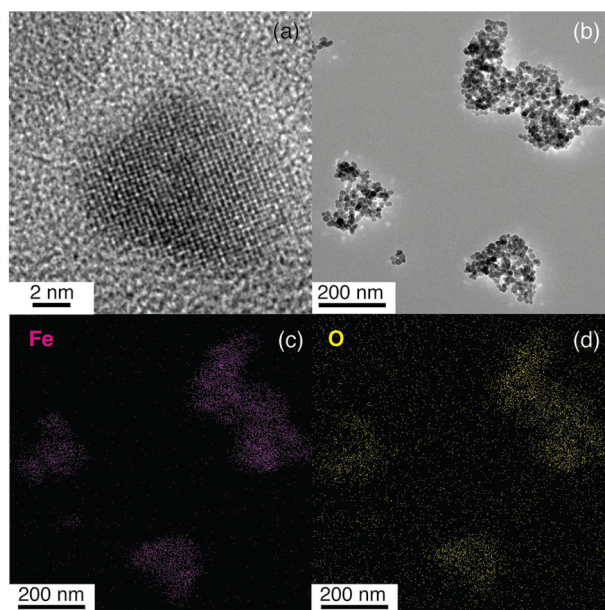
In this study, we used water-based ferrofluid containing superparamagnetic nanoparticles classified into the three types of EMG1111, EMG707 and EMG607 (Ferrotec, Japan) in line with different surface treatments. Table 1 shows characteristics of magnetic nanoparticles used in the experiment.

Table 1. Characteristics of magnetic nanoparticles used in the experiment.

	Particle Size	Composition	Appearance	Surface Treatment
EMG607	10 nm	$\text{Fe}_3\text{O}_4/\text{Fe}_2\text{O}_3$	Water-based ferrofluid	Cationic surfactant
EMG707				Anionic surfactant
EMG1111			Water-based slurry	No treatment

The surface of EMG1111 nanoparticles was not modified with any surfactant. In contrast, EMG707 nanoparticles were modified with an anionic surfactant to improve dispersion, and EMG607 nanoparticles were modified with a cationic surfactant. All the superparamagnetic nanoparticles had an average diameter of 10 nm, and were composed of mixtures of magnetite (Fe_3O_4) and maghemite (Fe_2O_3) iron oxides.

Figure 1. TEM images and EDS mapping images of EMG1111 magnetic nanoparticles. (a) TEM image of isolated magnetic nanoparticles; (b) TEM image of magnetic nanoparticles; (c) EDS mapping image of iron corresponding to image (b); (d) EDS mapping image of oxygen corresponding to image (b).



The characteristics of the superparamagnetic nanoparticles used in the experiments were examined using a transmission electron microscope (TEM) (JEM-2200FS, JEOL) and an energy-dispersive X-ray spectrometer (EDS) (JED-2300T, JEOL), as shown in Figure 1. The magnetic particle fluids were centrifuged to remove excess surfactant molecules. Additionally, the magnetic nanoparticle fluids were diluted to a certain concentration with distilled water, and the magnetic nanoparticles were then dispersed using ultra sonication.

Experimental PCR amplification is outlined here. The strain used in this study was *Escherichia coli* DH5a cultivated in LB medium. Cells were harvested by centrifugation and suspended in TEN buffer (10 mM Tris-HCl, pH 8.0, 1 mM EDTA, 100 mM NaCl), and 0.3 g of glass beads were added. The cells were broken by being shaken for 10 min on a vortex mixer at maximum speed, and nucleic acid was extracted through phenol/chloroform treatment and ethanol precipitation. An approximately 1,500-bp segment of the 16S rRNA gene was amplified by PCR with the forward and reverse primers 5'-AGA GTT TGA TCC TGG CTC AG-3' (positions 8–27 according to *Escherichia coli* numbering) and 5'-GGC TAC CTT GTT ACG ACT T-3' (positions 1510–1492) using an Ex Taq polymerase kit (TaKaRa). PCR thermal cycling was carried out in 0.2-ml reaction tubes in a QuickBath QB-0225A unit (ThermoGen Inc.). Amplification was performed in the following 50- μ L mixture: 5.0 μ L of 10 \times Ex Taq PCR buffer, 4.0 μ L of dNTP mixture (dATP, dTTP, dGTP and dCTP; 2.5 mM each), 1.0 μ L of forward primer, 1.0 μ L of reverse primer (10 mM each), 27.5 μ L of distilled water, 0.2 μ L of Ex Taq polymerase (1 U/ μ L), 1.0 μ L of template DNA (100 ng of DNA) and 10 μ L of ferromagnetic nanoparticles (EMG607: 0.4–1.8 μ g/ μ L; EMG707: 0.04–0.18 μ g/ μ L; EMG1111: 0.02–0.12 μ g/ μ L). The thermal profile for amplification began with an initial denaturation step (2 min, 96 °C) followed by 25 cycles of denaturation (20 s, 96 °C), annealing (20 s, 56 °C) and extension (90 s, 72 °C), then a final terminal extension step (2 min, 72 °C). Aliquots of 5.0 μ L from PCR were analyzed using agarose gel (1.2%) electrophoresis, and the product yield was confirmed using the InGenius system (Syngene).

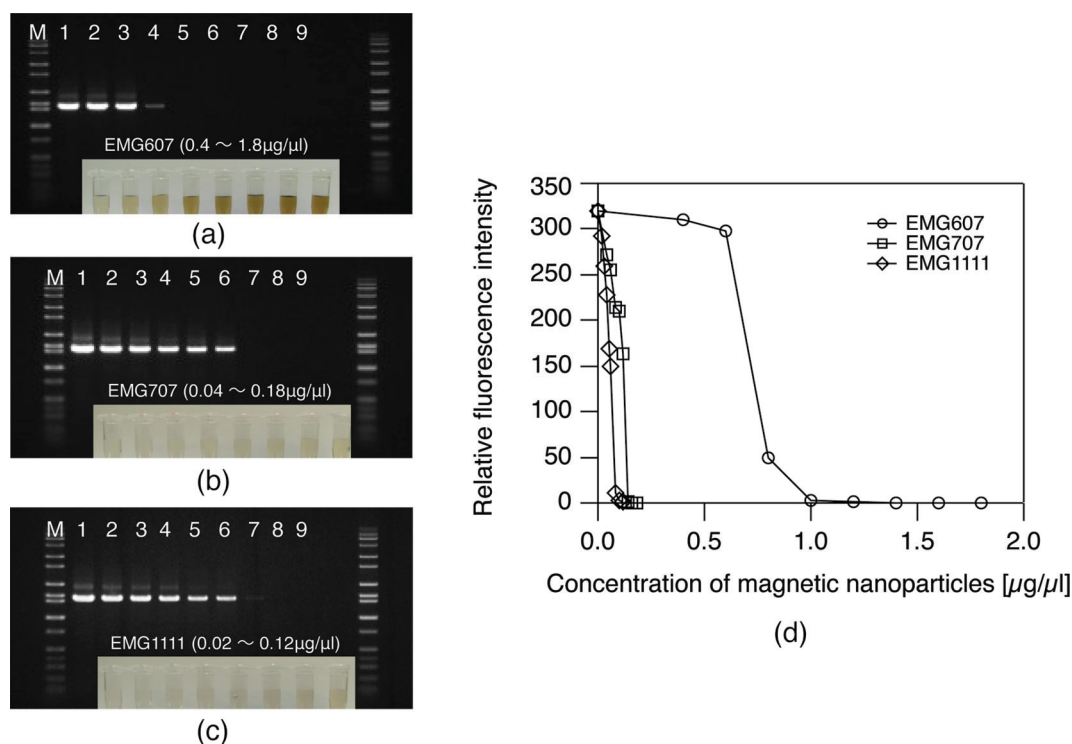
The structures of magnetic nanoparticle clusters were analyzed, and the interaction between PCR reagents and magnetic nanoparticle clusters in PCR was examined in the experiments outlined here. The distributions of the diameters of superparamagnetic nanoparticle clusters before and after heat treatment were measured using the dynamic scattering method (Zetasizer nano-zs, Malvern Instruments Ltd.). Additionally, the complex interaction between PCR reagents and nanoparticle clusters was analyzed in detail, using transmission electron micro-tomography (TEMT) (JEM2100, JEOL). The PCR reagents were then stained using the negative staining method with 2.0% uranyl acetate in order to scatter the TEMT electron beam.

3. Results and Discussion

First of all, we examined the effects of superparamagnetic nanoparticles on PCR amplification without an external magnetic field. Amplification was then performed while changing the concentration of the superparamagnetic nanoparticles mixed with the PCR reagent. Figure 2(a–c) show amplified DNA bands with different concentrations of magnetic nanoparticles observed using agarose gel electrophoresis. Each corresponds to the inset photograph of diluted magnetic nanoparticles with the same concentration. With EMG607 magnetic nanoparticles, PCR amplification was performed

with particle concentrations of 0.4–1.8 $\mu\text{g}/\mu\text{L}$. It was observed that the fluorescence intensity of DNA bands decreased with higher levels of nanoparticle concentration, and consequently PCR amplification was inhibited at higher concentrations, as shown in Figure 2(a).

Figure 2. Amplified DNA bands with different concentrations of magnetic nanoparticles observed using agarose gel electrophoresis, each corresponding to the inset photograph of diluted magnetic nanoparticles with the same concentration. (a) Lane 1: control without magnetic nanoparticles; lanes 2–9: 0.4, 0.6, 0.8, 1.0, 1.2, 1.4, 1.6 and 1.8 $\mu\text{g}/\mu\text{L}$ of EMG607 magnetic nanoparticles, respectively (b) Lane 1: control without magnetic nanoparticles; lanes 2–9: 0.04, 0.06, 0.08, 0.1, 0.12, 0.14, 0.16 and 0.18 $\mu\text{g}/\mu\text{L}$ of EMG707 magnetic nanoparticles, respectively (c) Lane 1: control without magnetic nanoparticles; lanes 2–9: 0.02, 0.03, 0.04, 0.05, 0.06, 0.08, 0.1 and 0.12 $\mu\text{g}/\mu\text{L}$ of EMG1111 magnetic nanoparticles, respectively. (d) Dependence of PCR product yield on the concentration of the magnetic nanoparticles added to the PCR solution.

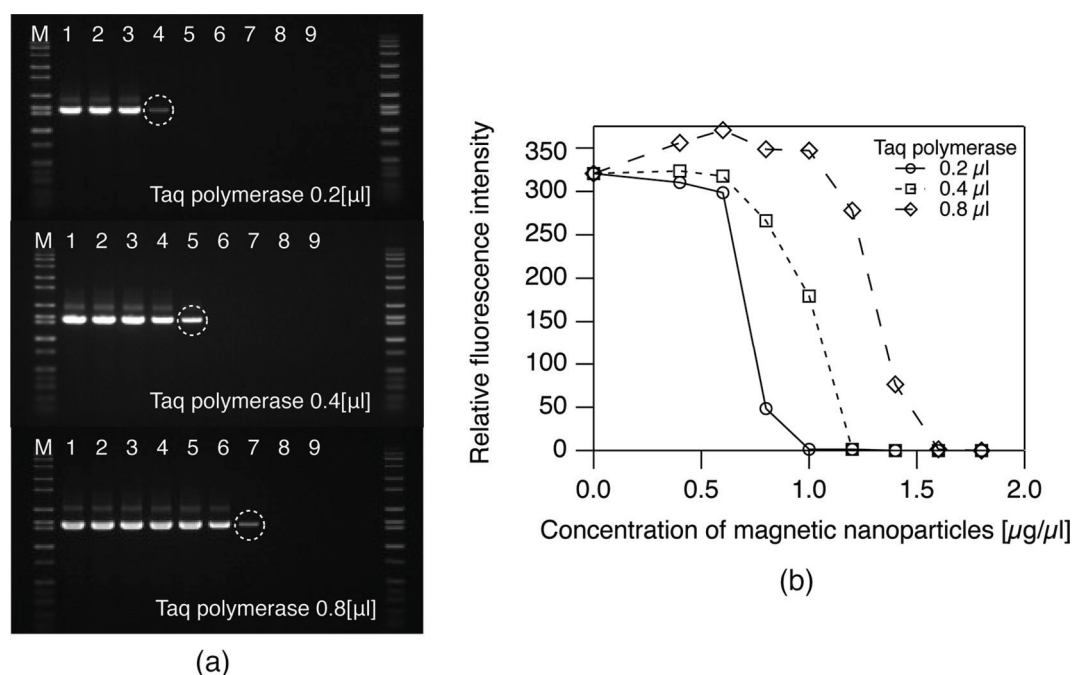


With EMG707 magnetic nanoparticles, PCR amplification was performed with particle concentrations of 0.04–0.18 $\mu\text{g}/\mu\text{L}$, and further amplification using EMG1111 magnetic nanoparticles was carried out with particle concentrations of 0.02–0.12 $\mu\text{g}/\mu\text{L}$. Magnetic nanoparticles of the EMG707 and EMG1111 types also inhibited PCR amplification at high concentrations, as shown in Figure 2(b,c). Figure 2(d) shows the dependence of product yield on the concentration of the magnetic nanoparticles added to PCR reagents in quantitative terms. It clearly indicates that the yield gradually decreased with higher levels of concentration, and as a result, PCR amplification was completely inhibited at threshold concentrations. The same figure also shows that the threshold concentrations for inhibited PCR amplification of EMG607, EMG707 and EMG1111 can be determined as 0.8, 0.12 and 0.08 $\mu\text{g}/\mu\text{L}$, respectively, and that threshold concentration strongly depends on the particle type.

EMG707 and EMG1111 magnetic nanoparticles have a low ratio of particles to PCR reagent and inhibit PCR amplification at low concentrations, while the EMG607 type with cationic surfactant modification has a high ratio of particles to PCR reagent and becomes effective at much higher concentrations. These results indicate that magnetic nanoparticles as well as gold nanoparticles suppressed PCR efficiency remarkably, thereby inhibiting PCR amplification. Consequently, we consider that an inhibitory effect is induced by complex interaction between nanoparticles and PCR reagents depending on particle surface properties.

To clarify the nature of the PCR inhibition effect, the influence of magnetic nanoparticles on specific PCR reagents was elucidated. As shown in Figure 3(a), PCR amplification with EMG607 magnetic nanoparticles is restored with increasing Taq polymerase concentrations of 0.4–0.8 $\mu\text{g}/\mu\text{L}$. Accordingly, when the concentration of the Taq polymerase increases, the inhibitory threshold concentration shifts to a higher level, as shown in Figure 3(b), and similar behavior is also observed when EMG707 or EMG1111 particles are used instead of the EMG607 type.

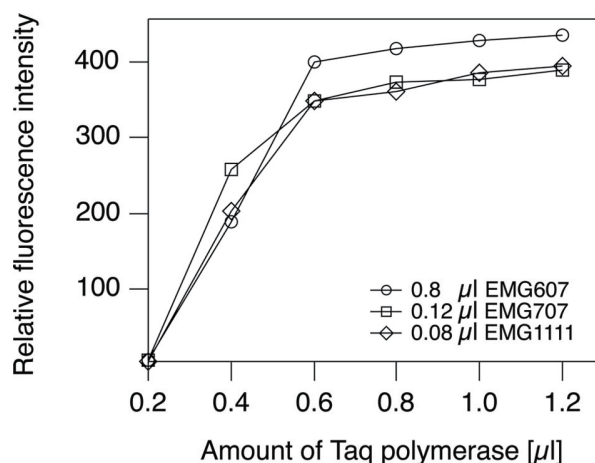
Figure 3. Amplified DNA bands with EMG607 magnetic nanoparticles having different amounts of Taq polymerase observed using agarose gel electrophoresis. Lane 1: control without magnetic nanoparticles; lanes 2–9: 0.4, 0.6, 0.8, 1.0, 1.2, 1.4, 1.6 and 1.8 $\mu\text{g}/\mu\text{L}$ of EMG607 magnetic nanoparticles, respectively. (a) The amounts of Taq polymerase used were 0.2–0.8 $\mu\text{g}/\mu\text{L}$; (b) Dependence of PCR product yield with EMG607 magnetic nanoparticles on amounts of Taq polymerase.



From the experimental results obtained, we found that only Taq polymerase of a DNA synthetic enzyme was sacrificed by magnetic nanoparticles, while other PCR components (such as the template DNA, both oligo primers and the deoxyribonucleotide triphosphate (dNTP)) were not sacrificed. The quantity of Taq polymerase used for PCR will decrease with an increase in the number of nanoparticles. Figure 4 also shows that all product yields were linearly enhanced by the addition of extra Taq polymerase at each threshold concentration, and as a result, all PCR amplifications were

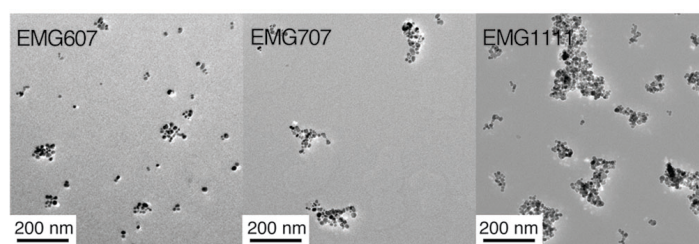
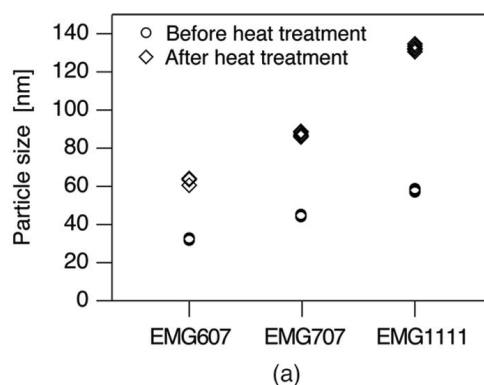
completely restored at a Taq polymerase concentration of 0.6 $\mu\text{g}/\mu\text{L}$. The same amounts of Taq polymerase that should have been used in PCR were sacrificed by the magnetic nanoparticles at each threshold concentration. In short, EMG707 and EMG1111 nanoparticles sacrificed the amounts of Taq polymerase more effectively than EMG607, although their threshold concentrations of EMG707 and EMG1111 were substantially lower than that of EMG607.

Figure 4. Dependence of PCR product yield with several types of magnetic nanoparticles at threshold concentration on amounts of Taq polymerase.



Next, we examined the state of magnetic nanoparticles in PCR solutions during PCR thermal cycles. The distributions of magnetic nanoparticle diameters were measured before and after heat treatment, as shown in Figure 5(a).

Figure 5. (a) Particle size distribution of EMG607, EMG707 and EMG1111 magnetic nanoparticles before and after heat treatment in PCR thermal cycles; (b) TEM image of EMG607, EMG707 and EMG1111 magnetic nanoparticles after heat treatment in PCR thermal cycles.

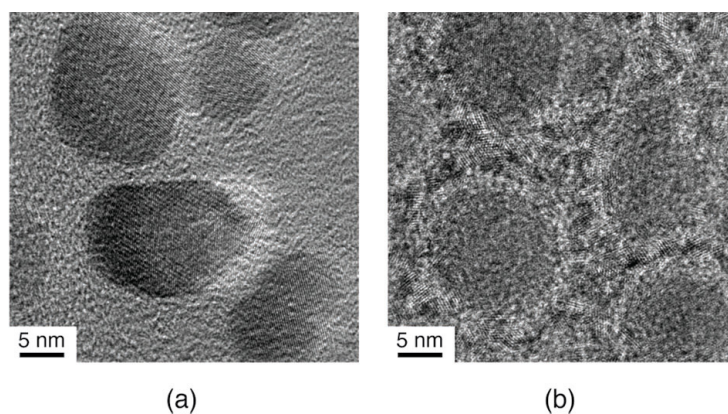


(b)

At room temperature without an external magnetic field, the magnetic nanoparticles EMG607, EMG707 and EMG1111 tend to aggregate to form clusters, and the size of clusters depends on surface properties of particles, although it is considered that superparamagnetic particles do not aggregate only by magnetic interactions. After the PCR thermal cycles, the size of the magnetic nanoparticle clusters was increased by heat treatment, regardless of their initial size. The heat treatment denatured the surface properties of the nanoparticles and then reduced their zeta potential, thereby promoting nanoparticle aggregation. Figure 5(b) shows TEM images of EMG607, EMG707 and EMG1111 magnetic nanoparticles after the PCR thermal cycles. It can be seen that they also aggregated to form irregular cluster structures. EMG707 and EMG1111 tended to strongly aggregate, and EMG1111 formed the largest clusters, while a considerable number of EMG607 magnetic nanoparticles remained stably dispersed. These results suggest a correlation between the size and shape of magnetic nanoparticle clusters and the concentration of the magnetic nanoparticles inhibiting PCR amplification.

We also analyzed the structure of EMG607 magnetic nanoparticle clusters heat-treated with the addition of Taq polymerase in PCR thermal cycles using TEM and TEMT. Figure 6(a) shows TEM images of EMG607 magnetic nanoparticle clusters heat-treated in these PCR thermal cycles without Taq polymerase. EMG607 magnetic nanoparticles formed tiny clusters with extremely small inter-particle spaces. Figure 6(b) shows TEM images of EMG607 magnetic nanoparticle clusters heat-treated in the PCR thermal cycles with 0.6 μL of Taq polymerase.

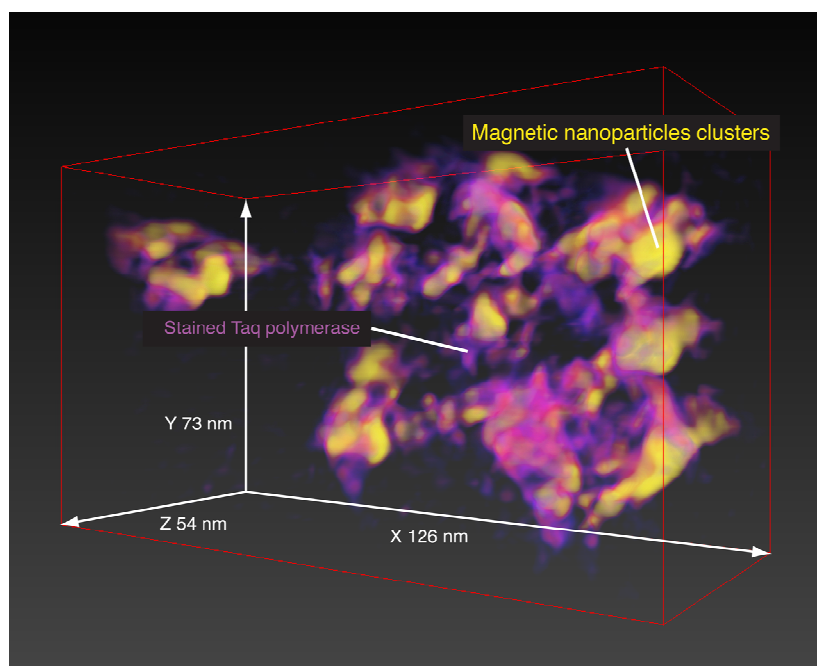
Figure 6. TEM images of EMG607 magnetic nanoparticle clusters heat-treated with the addition of Taq polymerase in PCR thermal cycles. (a) without Taq polymerase; (b) with 0.6 μL of Taq polymerase.



It can be seen that polymerase stained using the negative staining method was present in the spaces among the nanoparticles. These results suggest that a certain amount of Taq polymerase in the PCR solution was captured in the inter-particle spaces among magnetic nanoparticle formation clusters in the PCR thermal cycles. A TEMT 3D reconstruction image of EMG607 magnetic nanoparticle clusters heat-treated in the PCR thermal cycles with 0.6 μL of Taq polymerase is shown in Figure 7. Taq polymerase was then stained using the negative staining method with uranyl acetate, in order to scatter the electron beam. It can be seen that the surface of magnetic nanoparticles clusters were decorated with heavily stained Taq polymerase. Figure 7 illustrates that the Taq polymerase was also captured in the spaces among magnetic nanoparticles, although more was collected on the complex surfaces of magnetic nanoparticle clusters. We consider that heating-related thermal convection caused these

clusters to move, and that pristine Taq polymerase in the PCR solution was then collected by the effect of their motion *in vitro*. The aggregation and the motion effect of magnetic nanoparticles were therefore induced by heat treatment in the PCR thermal cycles, and as a result efficiently enhanced the capture of Taq polymerase by magnetic nanoparticle clusters in the PCR solution. These results indicate that magnetic nanoparticles with higher cohesion capture more Taq polymerase than those with good dispersibility, and that they have a stronger inhibitory effect on PCR amplification.

Figure 7. TEMT 3D reconstruction image of EMG607 magnetic nanoparticle clusters heat-treated in PCR thermal cycles with 0.6 μL of Taq polymerase.



These outcomes show that some amount of Taq polymerase is captured by magnetic nanoparticle clusters, and consequently, the amount of Taq polymerase that should have been used in PCR is reduced in the PCR solution. There are several reports on the effect of various nanoparticles on PCR amplification [2–10]. However, their reports did not focus on interaction between the particle clusters and Taq polymerase. Although the negative or positive effect of various nanoparticles on PCR amplification has been reported, the mechanism which causes these effects has never clarified. Wan *et al.* [10] concluded that the surfaces of individual gold nanoparticles and Taq polymerase bind to each other, and as a result, PCR amplification is inhibited, due to a reduction in the concentration of the free Taq polymerase in the PCR solution. They also suggested that larger gold nanoparticles have a stronger inhibitory effect on PCR amplification than smaller ones. In this way, the inhibitory effects of gold nanoparticles on PCR amplification are induced by interaction between individual gold nanoparticles and Taq polymerase. In contrast, we focused on the interaction between PCR reagents and magnetic nanoparticle clusters rather than individual magnetic nanoparticles. It is the first report clarifying the effect of the magnetic nanoparticle on PCR amplification, and also clarifying the mechanism behind the effects of superparamagnetic particle clusters on PCR efficiency from estimation of their structures in PCR thermal cycles. We revealed that magnetic nanoparticles formed cluster structures in PCR thermal cycles. The inhibitory effects of superparamagnetic nanoparticles on PCR amplification

strongly depend on their cluster sizes and structures. Therefore, we consider that the inhibitory effects of magnetic nanoparticles on PCR amplification is induced by interaction between Taq polymerase and magnetic nanoparticle clusters, rather than individual magnetic nanoparticles. The complex interaction between nanoparticles and PCR reagents is caused by the particle aggregation due to a decrease in particles dispersibility, and the mechanism behind such interactions will be helpful to understand similar interactions between polymerase and other nanoparticles. The present results also suggest that the effect of superparamagnetic particle clusters on PCR can be improved using an external magnetic field, and will be applied to novel PCR techniques in an external magnetic field. Additionally, using the external magnetic field, we have already demonstrated that the size, structure, and dynamics of particles clusters suppress PCR efficiency directly [21]. Therefore, our related report has justified the mechanism that we clarified in this paper. Those results also suggest that the effect of superparamagnetic particle clusters on PCR can be improved using various external magnetic fields, and will be applied to novel PCR models in various external magnetic fields. If such a field is applied, a magnetic dipole moment is induced in each particle, the magnetic particles form chain clusters, and consequently the size and the structure of the particle cluster can be controlled. Moreover, Kang *et al.* [22] simulated the chaotic mixing induced by a magnetic chain in a rotating magnetic field. Consequently, it can be considered that magnetic nanoparticles will work as a nano-size magnetic stirrer in the PCR process under an external varied magnetic field. This PCR technique could be applied to high frequency induction heating using AC magnetic fields.

4. Conclusions

We elucidated the effects of superparamagnetic nanoparticles on PCR amplification without an external magnetic field. It was found that such nanoparticles (like gold nanoparticles) suppressed PCR efficiency markedly, thereby inhibiting PCR amplification, and that the threshold concentration of particles strongly depends on their surface properties. We also found that superparamagnetic nanoparticles sacrificed Taq polymerase of a DNA synthetic enzyme in the same way as gold nanoparticles, reducing the concentration of the free polymerase in the PCR solution. However, it was also clarified that superparamagnetic nanoparticles and gold nanoparticles each exhibited different binding mechanisms for Taq polymerase. We focused on the interaction between magnetic nanoparticle clusters and Taq polymerase, and on the particle aggregation, depending on particle surface properties. We concluded that Taq polymerase in a PCR solution was captured in the spaces formed among magnetic nanoparticle clusters, depending on particle surface properties, and that it was captured more efficiently by the motion effect brought about in them by heat treatment in the PCR thermal cycles. Consequently, the amount of Taq polymerase that should have been used in PCR is reduced in the PCR solution. In the present study, superparamagnetic nanoparticles tended to suppress PCR amplification, but PCR efficiency could be enhanced using their outstanding specific magnetic properties in external magnetic fields.

Acknowledgments

This study was supported in part by a Grant for the High-Tech Research Centers organized by the Ministry of Education, Culture, Sports, Science and Technology (MEXT), Japan, from 2006 to 2010

and a Grant for the Strategic Development of Advanced Science and Technology organized by MEXT since 2011.

References

1. Saiki, R.K.; Gelfand, D.H.; Stoffel, S.; Scharf, S.J.; Higuchi, R.; Horn, G.T.; Mullis, K.B.; Erlich, H.A. Primer-directed enzymatic amplification of DNA with a thermo stable DNA polymerase. *Science* **1988**, *239*, 487–491.
2. Cui, D.; Tian, F.; Kong, Y.; Titushikin, I.; Gao, H. Effects of single-walled carbon nanotubes on the polymerase chain reaction. *Nanotechnology* **2004**, *15*, 154–157.
3. Zhang, Z.; Shen, C.; Wang, M.; Han, H.; Cao, X. Aqueous suspension of carbon nanotubes enhances the specificity of long PCR. *Biotechniques* **2008**, *44*, 537–542.
4. Zhang, Z.; Wang, M.; An, H. An aqueous suspension of carbon nanopowder enhances the efficiency of polymerase chain reaction. *Nanotechnology* **2007**, *18*, 355706.
5. Shen, C.; Yang, W.; Ji, Q.; Maki, H.; Dong, A.; Zhang, Z. NanoPCR observation: Different levels of DNA replication fidelity in nanoparticle-enhanced polymerase chain reactions. *Nanotechnology* **2009**, *20*, 455103.
6. Li, H.; Huang, J.; Lv, J.; An, H.; Zhang, X.; Zhang, Z.; Fan, C.; Hu, J. Nano particle PCR: Nanogold-assisted PCR with enhanced specificity. *Angew. Chem. Int. Ed.* **2005**, *44*, 5100–5103.
7. Li, M.; Lin, Y.C.; Wu, C.C.; Liu, H.S. Enhancing the efficiency of a PCR using gold nanoparticles. *Nucleic Acids Res.* **2005**, *33*, e-184.
8. Yang, W.; Mi, L.; Cao, X.; Zhang, X.; Fan, C.; Hu, J. Evaluation of gold nanoparticles as the additive in real-time polymerase chain reaction with SYBR Green I dye. *Nanotechnology* **2008**, *19*, 255101.
9. Vu, B.V.; Litvinov, D.; Willson, R.C. Gold nanoparticle effects in polymerase chain reaction: Favoring of smaller products by polymerase adsorption. *Anal. Chem.* **2008**, *80*, 5462–5467.
10. Weijie, W.; Yeow, J.T.W. The effects of gold nanoparticles with different sizes on polymerase chain reaction efficiency. *Nanotechnology* **2009**, *20*, 325702.
11. de Gennes, P.G.; Pincus, P.A. Pair correlations in a ferromagnetic colloid. *Phys. Kondens. Mater.* **1970**, *11*, 189–198.
12. Morimoto, H.; Maekawa, T. Cluster structure and cluster–cluster aggregations in a two dimensional ferromagnetic colloidal system. *J. Phys. A* **2000**, *33*, 247–258.
13. Promislow, J.H.E.; Gast, A.P.; Fermigier, M. Aggregation kinetics of paramagnetic colloidal particles. *J. Chem. Phys.* **1995**, *102*, 5492–5498.
14. Ukai, T.; Maekawa, T. Patterns formed by paramagnetic particles in a horizontal layer of a magnetorheological fluid subjected to a dc magnetic field. *Phys. Rev. E* **2004**, *69*, 032501.
15. Nagaoka, Y.; Morimoto, H.; Maekawa, T. Dynamics of disklike clusters formed in a magnetorheological fluid under a rotational magnetic field. *Phys. Rev. E* **2005**, *71*, 032502.
16. Morimoto, H.; Katano, K.; Maekawa, T. Ring-chain structural transitions in a ferromagnetic particles systems induced by a dc magnetic field. *J. Chem. Phys.* **2009**, *131*, 034905.

17. Mizuki, T.; Watanabe, N.; Nagaoka, Y.; Fukushima, T.; Morimoto, H.; Usami, R.; Maekawa, T. Activity of an enzyme immobilized on superparamagnetic particles in a rotational magnetic field. *Biochem. Biophys. Res. Commun.* **2010**, *393*, 779–782.
18. Pankhurst, Q.A.; Connolly, J.; Jones, S.K.; Dobson, J. Application of magnetic nanoparticles in biomedicine. *J. Phys. D: Appl. Phys.* **2003**, *36*, R167.
19. Tartaj, P.; del Puerto Morales, M.; Veintemillas-Verdaguer, S.; González-Carreño, T.; Serna, C.J. The preparation of magnetic nanoparticles for applications in biomedicine. *J. Phys. D: Appl. Phys.* **2003**, *36*, R182.
20. Berry, C.C.; Curtis, A.S.G. Functionalisation of magnetic nanoparticles for applications in biomedicine. *J. Phys. D: Appl. Phys.* **2003**, *36*, R198.
21. Higashi, T.; Nagaoka, Y.; Minegishi, H.; Echigo, A.; Usami, R.; Maekawa, T.; Hanajiri, T. Regulation of PCR efficiency with magnetic nanoparticles in a rotating magnetic field. *Chem. Phys. Lett.* **2011**, *506*, 239–242.
22. Kang, T.G.; Hulsén, M.A.; Anderson, P.D.; den Toonder, J.M.J.; Meijer, H.E.H. Chaotic mixing induced by a magnetic chain in a rotating magnetic field. *Phys. Rev. E* **2007**, *76*, 066303.

© 2012 by the authors; licensee MDPI, Basel, Switzerland. This article is an open access article distributed under the terms and conditions of the Creative Commons Attribution license (<http://creativecommons.org/licenses/by/3.0/>).